Version of Record: https://www.sciencedirect.com/science/article/pii/S0306261922008650
Manuscript_e7396143b07e348219b30ad78ffb1d76

Vehicle-to-manufacturing (V2M) System: A Novel Approach to Improve Energy Demand Flexibility for Demand Response towards Sustainable Manufacturing

Lingxiang Yun, Minkun Xiao, and Lin Li*

Department of Mechanical and Industrial Engineering, University of Illinois at Chicago, Chicago, IL 60607, USA
* Corresponding author. *E-mail address:* linli@uic.edu (L. Li).

Abstract:

The U.S. manufacturing sector accounts for 77% of the industrial energy consumption, but its participation in demand response (DR) programs is largely lagged behind. The relatively limited flexibility in production scheduling under high capacity utilization and the lack of DR schemes incorporating energy demand flexibility measures are deemed as major barriers. In this study, the framework of an interactive vehicles-to-manufacturing (V2M) energy sharing system is proposed to improve the energy demand flexibility of the aggregated system and enhance the DR effectiveness for manufacturers. The V2M-based DR scheme aims to reduce the energy cost by load shifting through joint production and energy sharing control, and it can eventually promote manufacturing DR implementation even under high capacity utilization requirements and dynamic real-time electricity prices. The V2M system is modeled based on a discrete-Markov chain considering the complex interconnections among various manufacturing resources and multi-directional energy flows among manufacturing facilities, electric vehicles, and the power grid. Based on the system model, a mixed-integer nonlinear programming (MINLP) problem is formulated to identify the optimal DR scheme. The effectiveness of the proposed approach is validated through comparisons with traditional manufacturing DR schemes. The results show that a 2.1 to 6.5 times energy demand flexibility improvement and an additional 4.7% to 6.9% energy cost reduction can be achieved by the proposed approach.

Keywords: Demand response; Electric vehicle; Energy demand flexibility; Real-time price; Smart grid; Sustainable manufacturing.

Nomenclature

Parameters	
$B_{n,t}$	Occupancy of the buffer n at time t
c	Heat capacity of air (kWh/kg ^{o}C)
c_t	RTP rate ($/kWh)
C_e	Cost of grid electricity ($)
C_{ev}	EV battery depreciation cost ($)
C_n	Maximum capacity of the buffer n
ec_t^H	Electricity consumption of the HVAC system at time t (kWh)
ec_t^M	Electricity consumption of the manufacturing system at time t (kWh)
$ef_t^{ev,mf}$	Energy flow from EVs to manufacturing facility at time t (kWh)
$ef_t^{grid,ev}$	Energy flow from power grid to EVs at time t (kWh)
$ef_t^{grid,mf}$	Energy flow from power grid to manufacturing facility at time t (kWh)
eff_n	Efficiency of machine n
GQ_t	Heat emission from the manufacturing system at time t (kWh)
k	Thermal conductivity of manufacturing facility
L	Average thickness of the walls and roofs (m)
p_i^{ev}	Unit depreciation cost ($/kW)
P_n	Rated power of machine n (kW)
PR_n	Production rate of machine n
PA	Production target
PT	Production throughput of the entire manufacturing system
Q_t	Energy required to maintain the indoor temperature (kWh)
Q_t^{io}	Heat transfers between the indoor and outdoor environment (kWh)
S	Surface area of the manufacturing facility (m^2)
$SOC_{i,t}$	SOC of the i-th EV's battery at time t
Tem_t^{in}	Indoor temperature at time t (^{o}C)
Tem_t^{out}	Outdoor temperature at time t (^{o}C)
Tem_t^{tar}	Target indoor temperature at time t (^{o}C)
V	Volume of the manufacturing facility (m^3)
Z_t	Operation state of the HVAC system
η^c	Cooling efficiencies of the HVAC system
η^h	Heating efficiencies of the HVAC system
η_{ev}^{ch}	EV charging efficiencies
η_{ev}^{disch}	EV discharging efficiencies
η_n	Energy efficiency of machine n
ρ	Density of air (kg/m^3)
Decision variables	
$x_{n,t}$	Binary variable deciding the operation state of the n-th machine at time t
$y_{i,t}$	Binary variable deciding the charging state of the i-th EV at time t
$z_{i,t}$	Binary variable deciding the discharging state of the i-th EV at time t
$P_{i,t}^{ch}$	Continuous variable controlling the charging power of the i-th EV at time t
$P_{i,t}^{disch}$	Continuous variable controlling the discharging power of the i-th EV at time t

1 Introduction

With the rapid development of smart grid technologies, the demand response (DR) is considered a promising strategy in promoting energy efficiency [1], reducing carbon emissions [2], and enhancing the energy distribution network's reliability and stability [3], [4]. The DR programs enable energy consumers to actively adjust their demand in response to the time-varying prices, reducing their energy cost while helping reshape the load profile and alleviate power grid congestion [5]. In particular, the manufacturing sector contributes 77% of the total industrial energy consumption in the U.S. in 2020 [6], and thus the DR schemes for manufacturing facilities have attracted widespread attention [7]–[9].

In the current literature, most DR studies for manufacturing facilities focus on the management of manufacturing systems. For example, Dababneh *et al.* proposed an analytical modeling-based approach for DR-driven production decision-making for serial production lines [10]. In addition, Lu *et al.* developed a data-driven DR scheme and validated it through a metal powder production line [11]. Recently, some studies extended these research efforts and considered other auxiliary systems in the manufacturing facility. For example, Sun *et al.* optimized the DR scheduling for combined manufacturing and heating, venting, and air-conditioning (HVAC) system [12]. Furthermore, Yun *et al.* proposed a DR scheme for manufacturing facilities considering the high power demand of the electric material handling equipment with fast charging stations [13]. Despite the impact of auxiliary systems on the total power demand, the manufacturing system is still the primary energy consumer and fundamentally determines the DR scheme. In general, the current DR schemes for manufacturing contribute to energy demand flexibility and load shifting/shedding by manufacturing system scheduling under production capacity utilization constraints, which adopted a foundational assumption that the capacity utilization rate of a manufacturing system should be limited, i.e., the desired production target should be significantly less than the maximum production throughput. Specifically, the capacity utilization rates in these DR studies are usually less than 70%. Otherwise, the effectiveness of load shifting/shedding in these DR schemes would be significantly diminished since the production line needs to be fully loaded even during some peak periods to achieve high production target.

However, this assumption is questionable in practice for industrials that require high capacity utilization rates. For example, to meet the increased chip demand, the semiconductor

manufacturers are substantially increasing their fab capacity utilization, especially under a worldwide “chips shortage” during the COVID-19 pandemic. The traditional DR schemes only consider the control of manufacturing resources, and thus the energy demand flexibility of the manufacturing facility is limited under high capacity utilization requirements. In addition, this flexibility issue is even more severe for the real-time price (RTP) based DR programs. Specifically, the RTP reflects the actual supply-demand relationship of the electricity market, which provides more benefit to the power system than the day-ahead price tariff in terms of reducing the peak demand and flattening the load profile, but it also requires a more flexible and timely DR control strategy [14]. Since the energy demand flexibility issue is hard to be addressed merely by production scheduling along, an energy storage system could potentially provide additional demand flexibility to manufacturing facilities [15]. In the current literature, integrating stationary energy storage systems with manufacturing systems, such as cement plant [16] and assembly plant [17], has been proved to be a feasible solution for demand flexibility improvement. However, stational energy storage systems require a vast capital investment, which may not be economically attractive to some manufacturers [18].

With the rapid growth of the electric vehicle (EV) market, the energy sharing between EVs and other energy systems presents a large potential to improve the aggregated energy demand flexibility with limited investment [19]. Hence, the energy sharing system with EVs could be a promising solution to the above-mentioned problem. Specifically, EVs in the smart grid are capable of not only drawing energy from the power grid, but also delivering energy to other systems to achieve the peak demand reduction of the aggregated energy system [20]. In the current literature, various research efforts have been devoted to DR schemes considering EVs in residential and commercial applications, which are referred to as Vehicle to Home (V2H) [21], [22] and Vehicle to Building (V2B) [23], [24]. Although these studies provide insights into the energy demand flexibility improvement for the aggregated system under DR, they cannot be directly integrated with manufacturing systems. In manufacturing systems, turning off one machine can potentially affect the operation status and the production throughput of the entire production line due to machine starvation and blockage [25]. In addition, the heat emission from machine operation can also affect the thermal load of the heating, ventilation, and air conditioning (HVAC) system [12]. Therefore, unlike the demand loads from appliances in V2H and V2B systems, which can be freely scheduled with limited constraints, the scheduling and

control of demand loads from machines, HVAC systems, and energy sharing between EVs and manufacturing facilities should be decided considering their complex interconnection. A DR scheme for manufacturing facilities that can reap the benefit of energy sharing system with EVs is still lacking.

To fill the above-mentioned research gap, a vehicle to manufacturing (V2M) energy sharing system and the V2M-based DR scheme are proposed in this study. The contributions of this study are summarized as follows.

1. The framework of the V2M system is proposed, where the EVs can provide electricity storage to manufacturing facilities for additional energy demand flexibility without compromising production capacity utilization under RTP-based DR program.
2. A discrete-time Markov decision process-based approach is applied to model the V2M energy sharing system, which systematically considers the impacts of production schedules and multidirectional energy interactions on production throughput and peak power demand.
3. A mixed-integer nonlinear programming (MINLP) optimization model is formulated and solved to find the optimal RTP-responsive DR scheme that can enhance the economic viability of the system.

The outcomes of this study provide a practical strategy to improve energy demand flexibility for manufacturers and allow them to reduce their energy costs even under high capacity utilization requirements through RTP-based DR programs.

The rest of this paper is organized as follows. In Section 2, the framework of the V2M system, system modeling, and optimization problem formulation are presented. The performance evaluation, comparative analyses, and sensitivity analyses of the proposed V2M-based DR scheme are discussed in Section 3. The conclusions and future work are provided in Section 4.

2 Proposed method

2.1 Description of V2M system

The V2M system enables energy sharing among the power grid, manufacturing facilities, and EVs. The framework of the proposed V2M energy sharing system is shown in Figure 1. More specifically, a V2M controller collects information such as RTP signals, manufacturing power

demand, and EV battery state of charge (SOC), and then optimizes the production scheduling and power flow within the system. In the manufacturing facility, the energy demands from the manufacturing system and heating, ventilation, and air conditioning (HVAC) system are considered in this study since these two systems are the largest energy consumers for direct process and direct non-process end uses in the U.S. manufacturing sector [26]. Machines in the manufacturing system consume energy for part fabrication, and the production schedule can be actively adjusted in response to RTP. The HVAC system consumes energy to maintain a desired indoor temperature. Due to the impact of heat emission from the machine operation on indoor temperature, the operation and energy consumption of the HVAC system are affected by the production schedule. EVs in the parking lot need to be charged to a desired battery level before departure, and their battery can be discharged to share the stored energy with the manufacturing facility. The EV charging/discharging activities are determined by controller after jointly considering the RTP and energy consumption of manufacturing facility. The possible energy flows and information flows in the proposed V2M system are represented by red lines and blue lines in Figure 1, respectively.

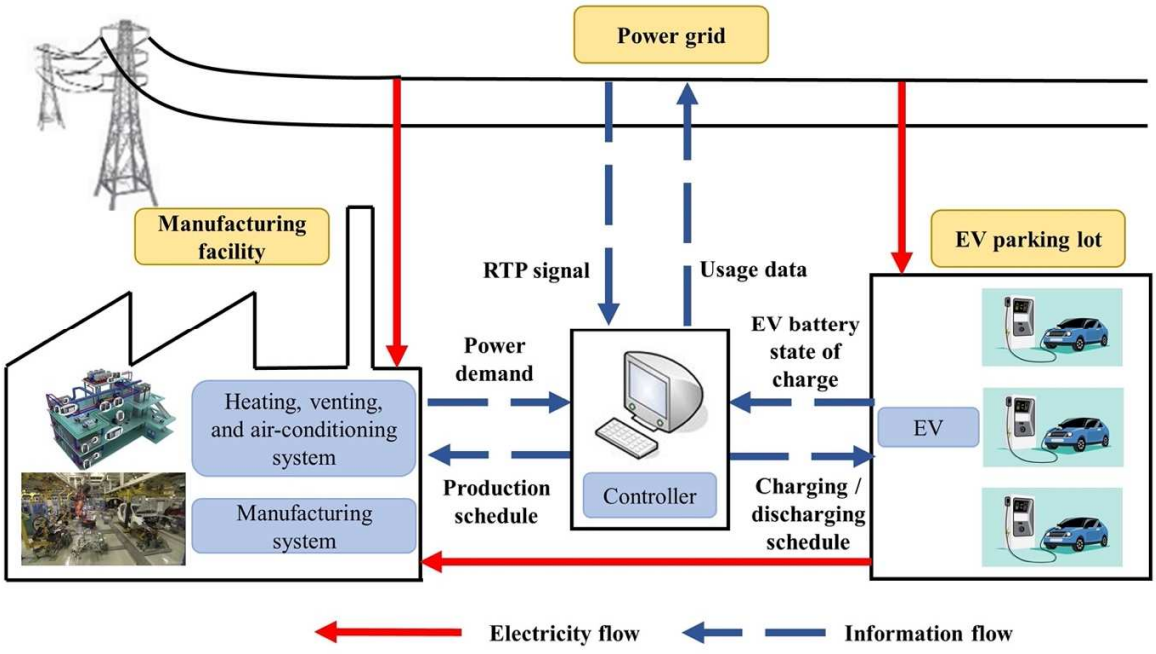

Figure 1. Framework of the proposed V2M energy sharing system.

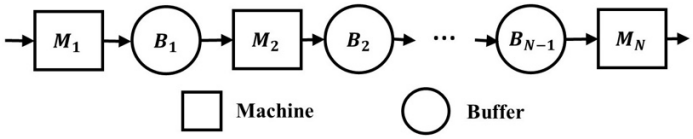

Figure 2. The layout of the manufacturing system.

In this study, the V2M energy sharing system is modeled based on a discrete-time Markov chain. The production horizon is evenly divided into T time slots, and the duration of each time slot $t \in [1, \dots, T]$ is Δt. The manufacturing system is represented by a serial production line with N machines and $N-1$ work-in-process buffers (as shown in Figure 2), and let n denote the index of machine and buffer. In addition, assume a total of M EVs are connected to the V2M system and let i denote the index of EV. In order to obtain the optimal control of the V2M system, three binary and two continuous decision variables are considered in this study. More specifically, binary variable $x_{n,t}$ decides the operation state of the n-th machine at time t; binary variables $y_{i,t}$ and $z_{i,t}$ determine the charging/discharging states of the i-th EV at time t, respectively. In addition, continuous variables $P_{i,t}^{ch}$ and $P_{i,t}^{disch}$ control the charging/discharging power of the i-th EV at time t, respectively. The binary decision variables are formally defined as follows:

$$x_{n,t} = \begin{cases} 1, & if\ the\ n^{th}\ mahcine\ is\ turn\ on\ at\ time\ t \\ 0, & otherwise \end{cases} \quad (1)$$

$$y_{i,t} = \begin{cases} 1, & if\ the\ i^{th}\ EV\ is\ charging\ at\ time\ t \\ 0, & otherwise \end{cases} \quad (2)$$

$$z_{i,t} = \begin{cases} 1, & if\ the\ i^{th}\ EV\ is\ discharging\ at\ time\ t \\ 0, & otherwise \end{cases} \quad (3)$$

The process of optimizing the production and energy sharing schedules and calculating the corresponding energy cost is shown in Figure 3. The models of manufacturing and HVAC systems in the manufacturing facility are discussed in Section 2.2.1, the EV charging/discharging model is presented in Section 2.2.2, and the optimization problem formulation is shown in Section 2.3. Note that since the actual RTP is not known at the scheduling stage, the price prediction is used to obtain the optimum schedule. Then, the actual RTP is applied to calculate the real energy cost and evaluate the optimal schedule.

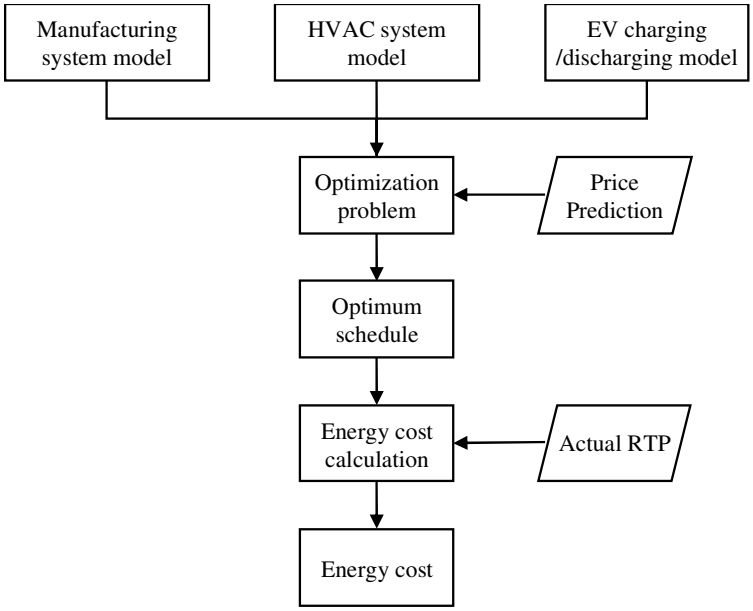

Figure 3. Flow chart of optimization and energy cost calculation.

2.2 V2M system modeling

2.2.1 Manufacturing facility

According to material balance, the buffer occupancy can be calculated as:

$$B_{n,t} = B_{n,t-1} + x_{n,t} \cdot PR_n \cdot eff_n \cdot \Delta t - x_{n+1,t} \cdot PR_{n+1} \cdot eff_{n+1} \cdot \Delta t \quad (4)$$

where $B_{n,t}$ is the buffer occupancy of the n-th buffer at time t; specifically, $B_{n,0}$ is the initial occupancy of the n-th buffer; PR_n is the production rate of the n-th machine (unit per hour); and eff_n is the efficiency of the n-th machine.

The production throughput (PT) of the entire manufacturing system is defined by the product processed by the last machine N,which can be calculated as:

$$PT = \sum_t x_{N,t} \cdot PR_N \cdot eff_N \cdot \Delta t \quad (5)$$

The electricity consumption of the manufacturing system, denoted by ($ec_t{}^M$), can be calculated as:

$$ec_t^M = \sum_n \left(x_{n,t} \cdot P_n \cdot \Delta t\right) \quad (6)$$

where P_n is the rated power of the n-th machine.

The heat emission from the manufacturing system (denoted by GQ_t) can affect the HVAC load to maintain the desired indoor temperature, which can be calculated by:

$$GQ_t = \sum_n x_{n,t} \cdot P_n \cdot \Delta t \cdot (1 - \eta_n) \tag{7}$$

where η_n is the energy efficiency of the n-th machine.

The heat transfers between the indoor and outdoor environment, denoted by Q_t^{io}, can be calculated as:

$$Q_t^{io} = k \cdot \frac{S}{L} \cdot \Delta t \cdot \left(Tem_t^{in} - Tem_t^{out}\right) \tag{8}$$

where k is the thermal conductivity of the walls and roofs of the facility; L is the average thickness of the walls and roofs; S is the surface area of the manufacturing facility; and Tem_t^{in} and Tem_t^{out} are indoor and outdoor temperature of the facility at time t, respectively. Note that the indoor-outdoor temperature difference determines whether Q_t^{io} is positive or negative.

The energy (Q_t) required to maintain the indoor temperature can be calculated as:

$$Q_t = c \cdot \rho \cdot V \cdot \left(Tem_t^{tar} - Tem_t^{in}\right) + Q_t^{io} - GQ_t \tag{9}$$

where c is the heat capacity of air; ρ is the density of air; V is the volume of the manufacturing facility; and Tem_t^{tar} is the target indoor temperature of the facility at time t.

Let Z_t denote the operation state of the HVAC system. Whether the HVAC system is in heating state ($Z_t = 1$) or cooling state ($Z_t = 0$) is determined by Q_t as:

$$Z_t = \begin{cases} 1, & if\ Q_t \geq 0 \\ 0, & otherwise \end{cases} \tag{10}$$

The electricity consumption of the HVAC system, denoted by (ec_t^H), can be calculated as:

$$ec_t^H = \frac{|Q_t|}{Z_t \cdot \eta^h + (1 - Z_t)\eta^c} \tag{11}$$

where η^h and η^c are the respective heating and cooling efficiencies of the HVAC system.

According to the conservation of energy, the total energy that flows into the manufacturing facility, i.e., from the power grid ($ef_t^{grid,mf}$) and EVs ($ef_t^{ev,mf}$), equals the energy consumed by manufacturing system and HVAC system.

$$ef_t^{grid,mf} + ef_t^{ev,mf} = ec_t^M + ec_t^H \tag{12}$$

2.2.2 EV changing/discharging

According to the conservation of energy, the EV battery state of charge (SOC) can be calculated as:

$$SOC_{i,t} = SOC_{i,t-1} + y_{i,t} \cdot P_{i,t}^{ch} \cdot \Delta t - z_{i,t} \cdot P_{i,t}^{disch} \cdot \Delta t \tag{13}$$

where $SOC_{i,t}$ represents the SOC of the i-th EV's battery at time t. Specifically, $SOC_{i,0}$ represents the initial SOC when the i-th EV arrives the parking lot.

The energy flows from EVs to the manufacturing facility and from the power grid to EVs ($ef_t^{grid,ev}$) are determined by the EV charging and discharging power, as shown in the following equations:

$$ef_t^{ev,mf} = \eta_{ev}^{disch} \cdot \sum_i P_{i,t}^{disch} \cdot z_{i,t} \cdot \Delta t \tag{14}$$

$$ef_t^{grid,ev} = \sum_i P_{i,t}^{ch} \cdot y_{i,t} \cdot \Delta t \,/\eta_{ev}^{ch} \tag{15}$$

where η_{ev}^{ch} and η_{ev}^{disch} are the respective charging and discharging efficiencies.

2.3 MINLP problem formulation

The MINLP problem can be formualted as:

$$\min_{x_{n,t}, y_{i,t}, z_{i,t}, P_{i,t}^{ch}, P_{i,t}^{disch}} \; COST = C_e + C_{ev} \tag{16}$$

$$s.t.\ 0 \le B_{n,t} \le C_n, \qquad \forall n, t \tag{17}$$

$$B_{n,0} = B_{n,T}, \qquad \forall n \tag{18}$$

$$PT \ge PA \tag{19}$$

$$y_{i,t} + z_{i,t} \le 1, \qquad \forall i, t \tag{20}$$

$$P_{ch}^{min} \le P_{i,t}^{ch} \le P_{ch}^{max}, \qquad \forall i, t \tag{21}$$

$$P_{disch}^{min} \le P_{i,t}^{disch} \le P_{disch}^{max}, \qquad \forall i, t \tag{22}$$

$$SOC^{min} \le SOC_{i,t} \le SOC^{max}, \quad \forall i, t \tag{23}$$

$$SOC_{i,T} \ge SOC^{dep}, \qquad \forall i \tag{24}$$

The objective of the optimization problem is to minimize the total cost of the V2M energy sharing system. The total cost includes two parts: the cost of grid electricity for the V2M system (C_e) and the EV battery depreciation cost (C_{ev}). The cost of grid electricity can be calculated as:

$$C_e = \sum_t c_t \cdot \left(ef_t^{grid,ev} + ef_t^{grid,mf}\right) \tag{25}$$

where c_t is the RTP at time t. Note that the predicted RTP is used for solving the optimization problem and find the optimal schedule since the actual RTP is not known in the day-ahead production scheduling stage. Whereas the actual RTP is applied to evaluate the obtained optimal solution.

The batteries in EVs usually have a fixed cycle life, i.e., the number of charge and discharge cycles that a battery can complete before losing performance [27]. Since EVs participating in the V2M system need to be charged and discharged more frequently, the batteries in these EVs are anticipated to have a shorter lifetime. Therefore, the EV owners should be paid for the battery depreciation, which can be estimated by the charging/discharging power as:

$$C_{ev} = \sum_i \left[p_i^{ev} \cdot \sum_t (P_{i,t}^{ch} + P_{i,t}^{disch}) \cdot \Delta t \right] \tag{26}$$

where p_i^{ev} is unit depreciation cost per kWh.

The first three constraints are related to the manufacturing facility. Constraint (17) shows that the occupancy of buffer n should be between zero and its maximum buffer capacity C_n. Constraint (18) shows that the buffer occupancy before and after the production horizon should maintain the same level to ensure long-term production stability. Constraint (19) represents the product throughput requirement, i.e., the throughput should be no less the desired production target (denoted by PA).

The rest five constraints are related to the EV charging/discharging activities. Constraint (20) indicates that an EV cannot be charged and discharged at the same time. Constraints (21) and (22) define the charging/discharging power limits, where P_{ch}^{min} and P_{ch}^{max} are minimal and maximal allowed charging power, respectively; and P_{disch}^{min} and P_{disch}^{max} are minimal and maximal allowed discharging power, respectively. Constraint (23) shows that batteries cannot be overcharged or overdischarged, i.e., the battery SOC should be in a range from SOC^{min} to SOC^{max}. The last constraint indicates that EV should be charged to a desired battery level (denoted by SOC^{dep}) before departure.

3 Results and discussions

3.1 Case study settings

In this study, the manufacturing system is assumed to be a five-machine-four-buffer serial production line. All machine-related parameters, i.e., production rate, power, and energy efficiency, are listed in Table 1. In addition, the buffer-related parameters, i.e., initial buffer occupancy, and maximum buffer capacity, are listed in Table 2. The production horizon is set to

an eight-hour shift from 9:00 to 17:00. The production horizon is evenly divided into 32 time slots, and the length of each time slot Δt is 15 min.

The manufacturing facility is assumed to be a building whose floor area is 40m by 40m and the height is 10m. The thermal conductivity of the walls and roofs of the facility is 0.001695 kW/m ºC [28]. The specific heat capacity of air is 0.00028 kWh/kg ºC. The target indoor temperature of the manufacturing facility is set to be 20 °C, and the outdoor temperature is adopted from the recent weather records in New York [29]. The cooling and heating efficiencies of HVAC are assumed to be 70% and 80%, respectively.

Table 1. Machine parameters

Machine	Production rate (unit/h)	Power (kW)	Energy efficiency
M1	40	60	0.85
M2	40	80	0.85
M3	40	100	0.80
M4	40	100	0.85
M5	40	80	0.80

Table 2. Buffer parameters

Buffer	Initial occupancy	Maximum capacity
B1	20	80
B2	20	80
B3	25	100
B4	20	80

In this study, the EV battery capacity is set to be 30 kWh, and both charging/discharging efficiencies are set to be 95% [30]. Forty EVs are assumed to arrive at the parking lot at the beginning of the production horizon with different battery levels. Specifically, it is assumed that twenty EVs arrive with a low battery level (20%), and the other twenty EVs arrive with a high battery level (50%). All EVs are assumed to depart the parking lot at the end of the production horizon with the minimum required departure battery level of 80%. The minimum charging/discharging rates are assumed to be 2kW. The maximum charging/discharging rates are

respectively set to 19.2kW and 9.6kW based on Ford charge station pro [31]. The depreciation cost for EV batteries is assumed to be ₵0.25/kWh [32].

The actual RTP is adopted from New York Independent System Operator (NYISO) [33], whereas the predicted RTP is obtained using long short-term memory (LSTM). LSTM is an artificial recurrent neural network architecture specialized for processing sequential data, which is widely used in problems such as speech recognition and market price trend prediction. The actual and predicted RTPs used in this study are shown in Figure 4. The predicted RTP is used for MINLP formulation, and the actual RTP is applied to evaluate the optimal production schedule. The optimization problems are solved using LINGO on a laptop with an Intel® Core™ i7 CPU and an 8 GB memory, and the optimality tolerance in LINGO is set to 10^{-5}.

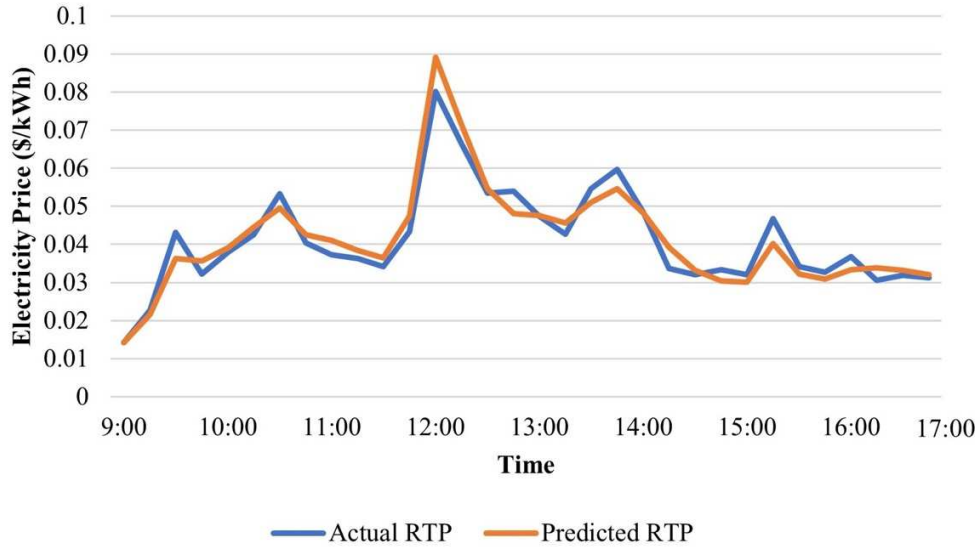

Figure 4. Actual RTP and predicted RTP on Dec. 19, 2020.

In this study, three scenarios are established and compared to evaluate the effectiveness of the proposed V2M system in improving the energy demand flexibility in manufacturing facilities and reducing energy cost for manufacturers. The details of three scenarios are described as follows:

1) Scenario I (baseline): in this scenario, the manufacturing facility and EVs are controlled independently. In addition, the manufacturing facility control strategy aims to minimize electricity consumption, i.e., the RTP-based DR program is not considered in this scenario.

2) Scenario II (without V2M): in this scenario, the traditional manufacturing DR control method is adopted, where the manufacturing facility is controlled independently in response to RTP without energy sharing between EVs and manufacturing facility (ensured by the following equation).

$$P_{i,t}^{disch} = 0 \tag{27}$$

3) Scenario III (with V2M): in this scenario, the proposed V2M system is applied for DR control, i.e., the EVs can share energy with manufacturing facility to achieve the minimum energy cost of the entire V2M system under DR.

3.2 Performance evaluation of the proposed V2M energy sharing system

In this subsection, the superiority of the proposed V2M system in energy demand flexibility improvement and energy cost reduction are evaluated and compared with the other two scenarios under various production targets (capacity utilization rates). More specifically, the maximum production throughput of the manufacturing system in case studies is 320, i.e., the production throughput achieved when all machines are turned on during the entire production horizon (the capacity utilization rate is 100%). Five production targets (capacity utilization rates), from 240 (75%) to 320 (100%), are evenly selected for performance evaluation. The MINLP problem under each case setting is solved five times, and the calculation takes around 3.8 seconds. The solutions in all five trials converge to the same value.

The energy demand flexibilities are represented by two metrics from different aspects, i.e., the quantitative metric (E_{fle}) showing the amount of energy that can be shifted during the production horizon, and the temporal metric (t_{fle}) showing the total duration of the shifted energy demand [34]. These two metrics can be calculated as follows:

$$E_{fle} = \sum\nolimits_t \max\left(0, ec_t^{base} - ec_t^{DR}\right) \tag{28}$$

$$t_{fle} = \Delta t \cdot \left|\{t | ec_t^{base} - ec_t^{DR} > 0\}\right| \tag{29}$$

where ec_t^{base} is the energy demand from the power grid at time t in baseline scenario (Scenario I), and ec_t^{DR} is the energy demand from the power grid at time t in DR control scenario (Scenarios II and III). The comparison of energy demand flexibilities in Scenarios II and III are shown in Table 3.

Table 3. Energy demand flexibility comparison

Production target (capacity utilization)	E_{fle} **(kWh)**		t_{fle} **(h)**	
	Scenario II	**Scenario III**	**Scenario II**	**Scenario III**
240 (75.0%)	647.81	1385.93	2.00	2.75
260 (81.3%)	474.69	1319.99	1.50	2.75
280 (87.5%)	330.00	1202.94	1.00	2.75
300 (93.8%)	165.00	1077.00	0.50	2.50
320 (100.0%)	0	912.00	0	2.50

The results show that in the case of 100% capacity utilization, the energy demand flexibilities represented by two metrics are equal to zeros under the traditional DR scheme in Scenario II, whereas the proposed V2M-based DR scheme can still ensure decent levels of energy demand flexibility. In the other four cases, compared to Scenario II, the proposed approach in Scenario III can improve the metric E_{fle} by 2.1 to 6.5 times and the metric t_{fle} by 1.4 to 5 times.

In addition, the costs achieved in Scenario I are treated as baseline costs (100%). The costs achieved in Scenarios II and III are compared to the baseline costs, and the results are shown in Figure 5. The results show that the proposed V2M-based DR scheme outperforms the traditional DR scheme under all five cases. Specifically, Scenario III can further reduce the total cost by 4.7% to 6.9% compared to Scenario II. In addition, the results in Figure 5 show that the cost reduction effect under DR control diminishes with increasing capacity utilization. Specifically, the cost reductions achieved by traditional method in Scenario II are reduced from 10.5% when capacity utilization is 75% to 0% when capacity utilization is 100%. Since the traditional method can only adjust the machine operation schedule to avoid the electricity peak period, this method loses effectiveness when machines must be in operation state for a longer time to achieve a higher capacity utilization. Especially under the 100% capacity utilization, the traditional method is completely invalid. In comparison, since the proposed V2M-based DR scheme provides more energy demand flexibility, the total cost can still be reduced by 6.9% through the energy sharing between the manufacturing facility and EVs even under the highest capacity utilization.

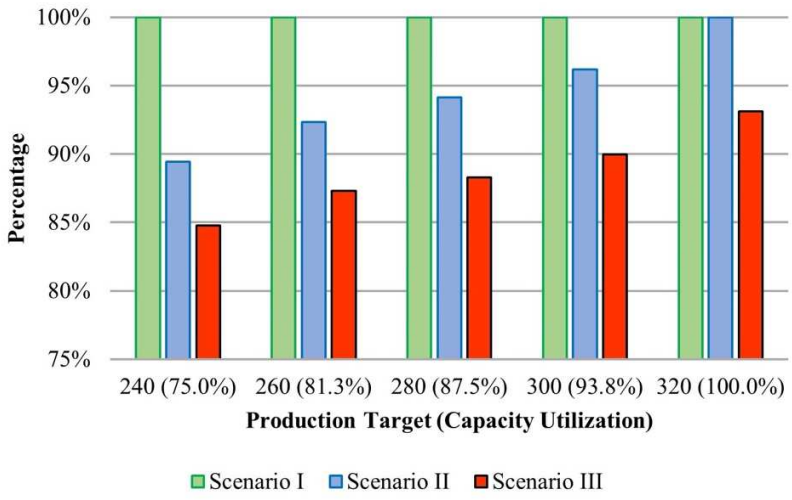

Figure 5. The cost percentage of three scenarios compared with Scenario I under five different capacity utilization rates.

Specifically, the details of production schedules, EV charging/discharging activities, power demands, and cost analysis under the production target 300 (93.8% capacity utilization) are discussed next as an example to show the difference between the traditional method in Scenario II and the proposed method in Scenario III.

Figure 6 shows the optimal production schedules obtained in Scenarios II and III. The results indicate that production schedules tend to avoid high electricity prices during peak periods in both two scenarios. More specifically, since production schedule adjustment is the only mechanism responding to peak demand in Scenario II, all five machines are turned off from 12:00 to 12:30 to avoid the highest electricity price, as shown in Figure 6 (a). However, in order to achieve high capacity utilization, machines can only be turned off for a limited time. Hence, the production schedule in Scenario II cannot respond to other peak periods, such as the period from 13:30 to 14:15 (as shown in Figure 4). In comparison, Figure 6 (b) shows a more flexible DR control method in Scenario III. Specifically, attributed to the energy sharing between EVs and the manufacturing facility, machines can use electricity from EVs instead of from the power grid during peak periods. Therefore, in this scenario, manufacturers can turn some machines on from 12:00 to 12:30 without paying for the highest RTP. Consequentially, machines can be turned off during other periods in response to more peak electricity price while satisfying high capacity utilization.

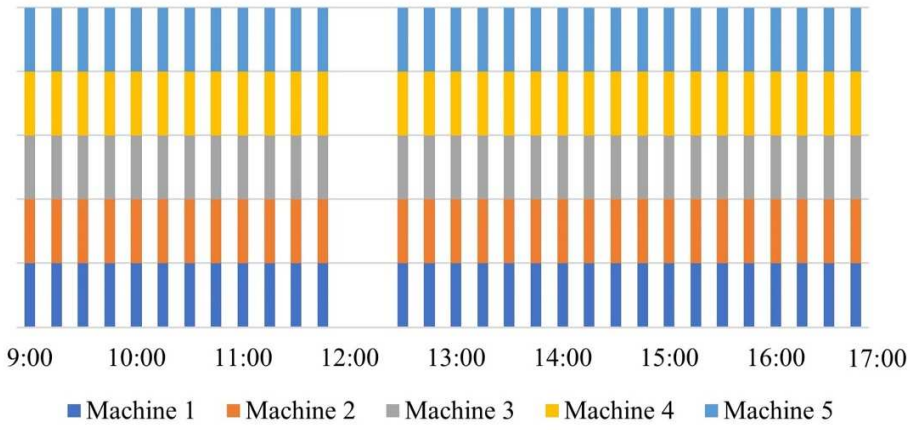

(a)

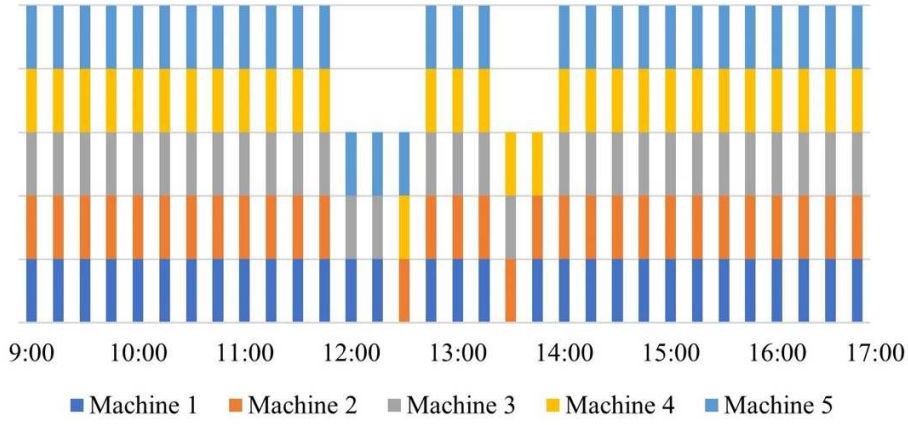

(b)

Figure 6. The optimal production schedules in (a) Scenario II and (b) Scenario III.

The changes in power demands of manufacturing and HVAC systems in Scenario III are shown in Figure 7. Specifically, results in Figure 7 (a) show that the manufacturing power demand is reduced by 140 to 180 kW during two peak periods based on the production schedule in Figure 6 (b). In addition, the power demand of the HVAC system reacts to the outdoor temperature and electricity price, and the results are shown in Figure 7 (b). Since the temperature data on a winter day is applied in this case, the HVAC system is used to warm up the manufacturing facility. Therefore, in general, the power demand of the HVAC system decreases with the increasing outdoor temperature. In addition, since the power demand of the manufacturing system is reduced during two peak periods, the heat emission from the

manufacturing system is also reduced during these periods. Therefore, the HVAC system should consume more energy to keep the desired indoor temperature during these two periods. Although the power demand of the HVAC system increases by 30 kW to 45 kW during peak periods, considering the demand reduction of the manufacturing system, the total power demands of the manufacturing facility are still reduced by 95 to 150 kW during peak periods based on the proposed DR scheme.

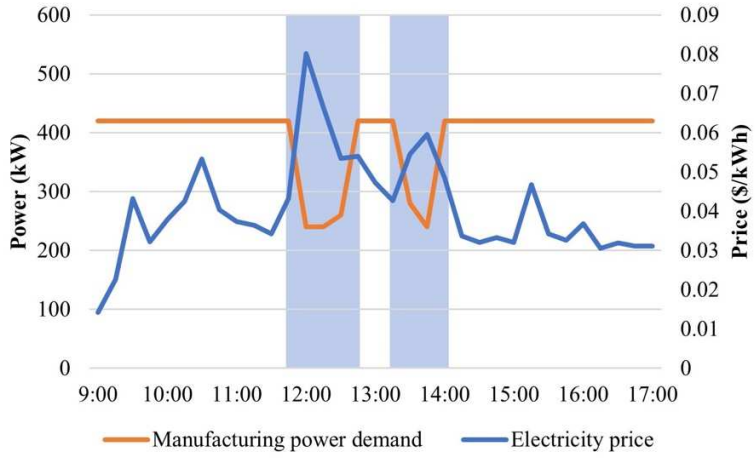

(a)

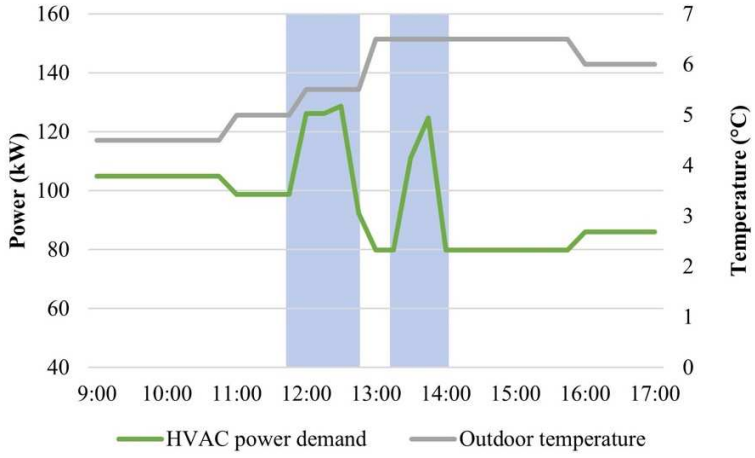

(b)

Figure 7. The changes in power demands of manufacturing and HVAC systems due to DR in Senario III.

The EV charging and discharging power shown in Figure 8 further explains the reason for the differences between two production schedules. As shown in Figure 8 (a), since there is no energy sharing in Scenario II, EVs only charge twice during off-peak periods to ensure 80% of battery level before departure. On the contrary, in Scenario III, EVs need to charge more frequently during off-peak periods to store enough electricity for energy sharing. Consequently, as shown in Figure 8 (b), EVs are able to discharge and share the stored energy with the manufacturing facility during three peak periods, i.e., around 10:30, from 11:45 to 13:15, and from 13:30 to 14:15. Combining the energy sharing and manufacturing scheduling, the proposed V2M system can help manufacturers reduce power demand from the grid during all three peak periods even under high capacity utilization.

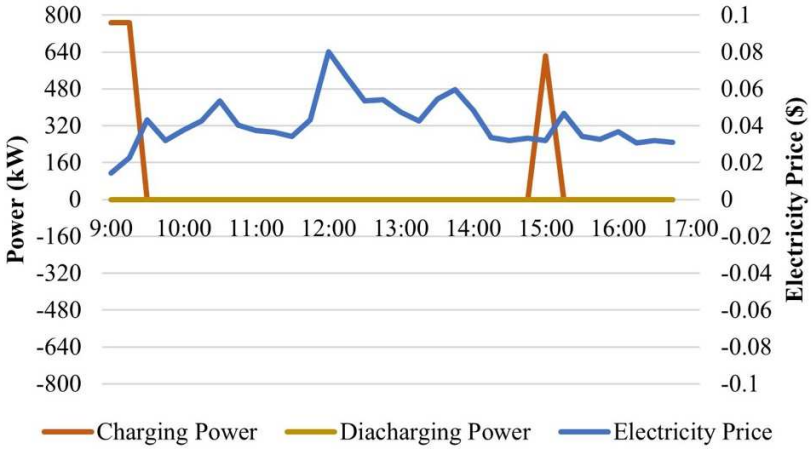

(a)

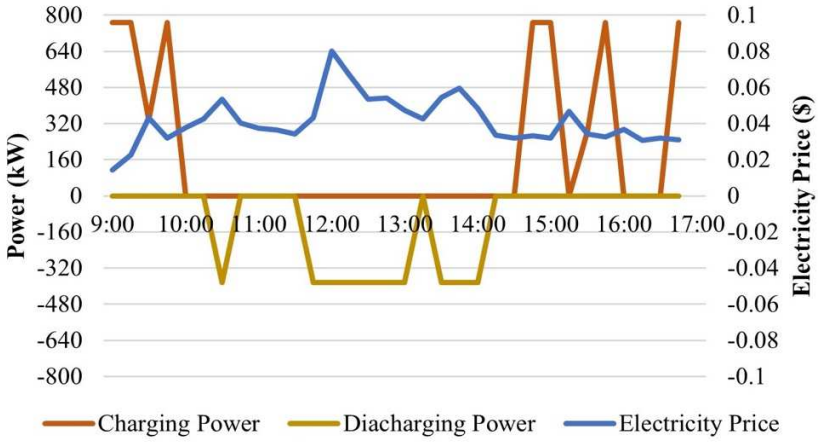

(b)

Figure 8. The charging and discharging power of EVs in (a) Scenario II and (b) Scenario III.

Figure 9 shows the total power demand required from the grid in Scenarios II and III. The results indicate that the traditional method in Scenario II can only respond to one peak period from 12:00 to 12:30 under high capacity utilization. However, due to the energy consumption of the HVAC system, the manufacturing facility still needs 183 kW from the grid during this period, even if all five machines are temperately turned off. In comparison, the V2M-based DR scheme in Scenario III is more flexible. The V2M system can respond to all three peak periods and significantly reduce the power demand from the grid during these periods. In general, the V2M system can shift the power demand from peak periods to off-peak periods. Therefore, it can eventually alleviate congestion on the power system and help manufacturers reduce energy cost.

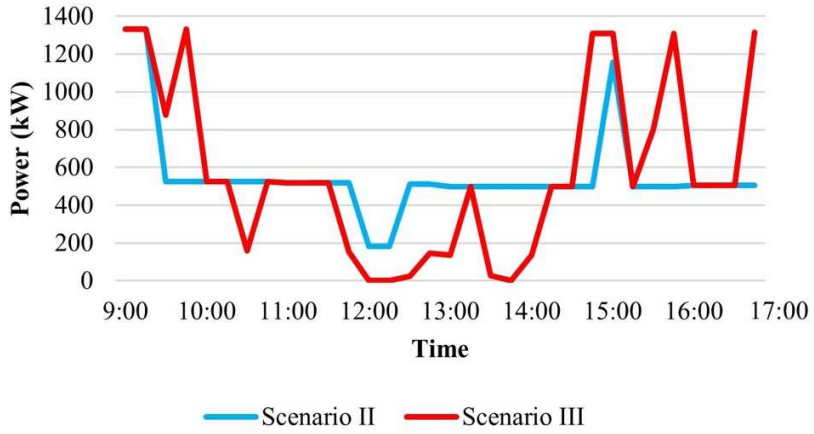

Figure 9. Total power demand from the grid in Scenario II and Scenario III.

The detailed energy and cost comparisons between Scenarios II and III are presented in Table 4. Compared with Scenario II, the manufacturing facility in Scenario III is less dependent on the grid, and its electricity consumption is significantly reduced by 23.3%. At the same time, the EVs in Scenario III consume more electricity from the grid for energy sharing, which results in a slightly higher total electricity consumption (i.e., 2.2% in this case). In addition, due to the frequent EV charging and discharging, the EV battery cost in Scenario III is also higher than Scenario II. However, even though Scenario III is associated with slightly higher total electricity consumption and battery cost, it successfully reduces power demand during peak periods. As a

result, the proposed V2M-based DR scheme eventually reduces the electricity and total costs by 9.4% and 6.5% than the traditional manufacturing DR scheme.

Table 4. The energy and cost comparisons between Scenarios II and III

	Electricity consumption from the grid (kWh)			EV battery	Electricity	Total
	Manufacturing facility	EVs	Total	cost ($)	cost ($)	cost ($)
Scenario II	3921.70	568.42	4490.12	1.35	169.08	170.43
Scenario III	3009.70	1578.95	4588.65	6.15	153.27	159.42
Decrease					9.4%	6.5%

3.3 Comparative analyses

In this subsection, the performance of the proposed V2M-based DR scheme is compared with some other rule-based energy sharing schemes [35], [36], in which the manufacturing system scheduling is not jointly optimized with the EV energy sharing. Specifically, the alternative schemes include price-based method without facility power demand information (PBWO), price-based method with facility power demand information (PBW), time-based method without facility power demand information (TBWO), and time-based method with facility power demand information (PBW). In the four alternatives, the EV charging/discharging timing is only determined by the power grid signals. In two price-based methods, EVs discharge and share energy with the manufacturing facility when the predicted RTP is higher than a predefined threshold. Whereas in two time-based methods, EVs discharge during a fixed period. In all four alternatives, EVs are charge during off-peak periods. In addition, if the manufacturing facility's power demand information is not available, EVs discharge at the maximum power; otherwise, EVs discharge to meet the power demand of manufacturing facility. In this study, the threshold for price-based methods is set to 70% of the maximum predicted RTP during production horizon. The fixed discharging period for time-based methods is set to 13:00 to 14:00, which is a typical peak period according to the RTP record [33]. The comparison results among five control methods are represented in Figure 10. This figure shows that the proposed method outperforms all other alternatives and achieves the lowest total cost under five production targets. This result indicates the necessity of the proposed V2M-based DR scheme, i.e., jointly considering the

manufacturing system scheduling and EV energy sharing, in obtaining the optimal DR control for manufacturers.

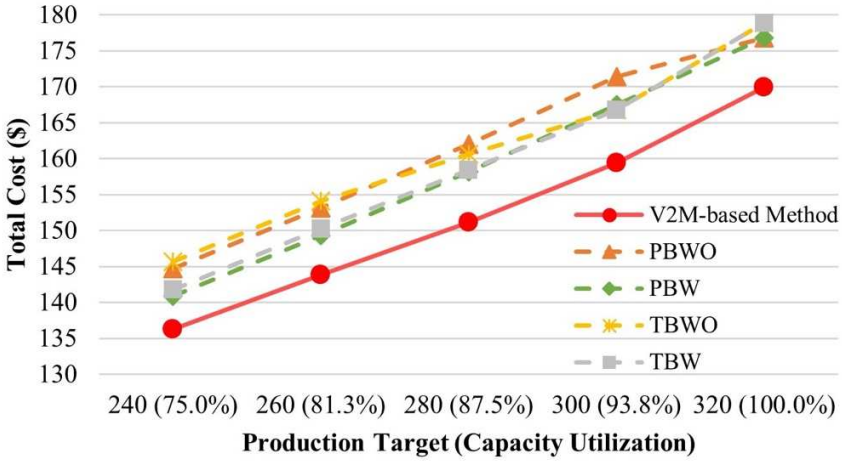

Figure 10. The total cost comparison between the proposed V2M-based DR scheme and four alternatives.

3.4 Sensitivity analyses

In this subsection, sensitivity analyses are conducted to test the proposed V2M-based DR scheme under various RTPs and EV settings. Specifically, three RTPs in summer (denoted by S-1, S-2, and S-3) and three RTPs in winter (denoted by W-1, W-2, and W-3) are selected to test the robustness of the proposed scheme. Each selected RTP has different peak periods and patterns, as shown in Figure 11. The production target (capacity utilization) is set to 300 (93.8%). The comparisons of energy demand flexibilities and total costs are shown in Tables 5 and 6, respectively.

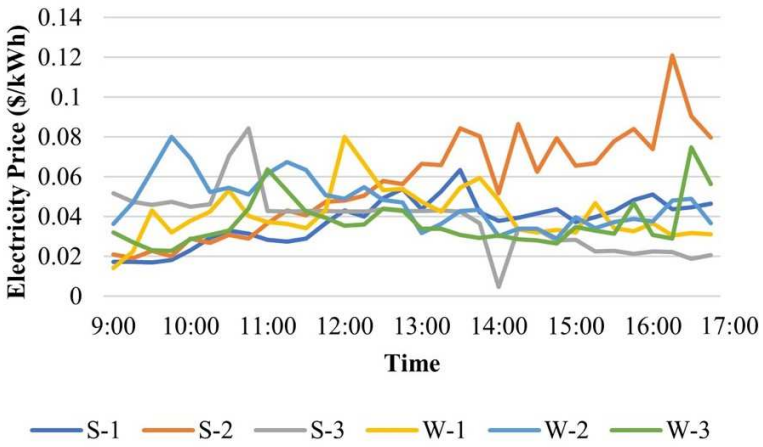

Figure 11. The six RTPs for sensitivity analysis.

Table 5 shows that the system always has larger energy demand flexibility in Scenario III. Specifically, the flexibility metric E_{fle} in Scenario III is improved by 3.3 to 6.5 times comparing to Scenario II. The metric t_{fle} is also improved by 3 to 5.5 times.

Table 5. Energy demand flexibility comparison under different RTPs

	E_{fle} (kWh)		t_{fle} (h)	
	Scenario II	**Scenario III**	**Scenario II**	**Scenario III**
S-1	261.43	1173.43	0.50	2.75
S-2	229.29	749.89	0.50	1.50
S-3	235.71	962.40	0.50	2.25
W-1	165.00	1077.00	0.50	2.50
W-2	127.50	834.73	0.50	2.00
W-3	150.00	886.81	0.50	2.25

The results in Table 6 show that under all six RTPs, the total costs in Scenario III are always the lowest. More specifically, in Scenario III, the total costs are reduced by 7.53% to 10.20% compared to baseline in Scenario I, which means costs are further reduced by 3.37% to 6.21% compared to the traditional method in Scenario II. The results validate the robustness of the proposed DR schemes under different RTPs.

Table 6. Total cost comparison under different RTPs

Scenario I	**Scenario II**	**Scenario III**

	Cost	Decrease	Cost	Decrease	Cost	Decrease
S-1	204.89	-	194.16	5.24%	183.99	10.20%
S-2	222.08	-	213.02	4.08%	203.83	8.22%
S-3	209.12	-	200.42	4.16%	193.37	7.53%
W-1	177.21	-	170.43	3.83%	159.42	10.04%
W-2	204.05	-	199.32	2.32%	188.26	7.74%
W-3	160.01	-	154.44	3.48%	146.31	8.56%

In addition, the impacts of two EV-related factors (i.e., quantity of EV and battery depreciation cost) on the performance of the proposed approach are investigated.

The quantity of EV is one of the most critical factors affecting the total cost. Specifically, the EV quantity directly determines the maximum energy flow from EVs to the manufacturing facility, and thus it affects the energy sharing ability of the V2M system. As shown in Figure 12, the effectiveness of total cost reduction improves as the EV quantity increases. However, the impact of increasing EV quantity on cost reduction is diminished after the number of EVs exceeds a threshold. For example, if the battery depreciation charge equals ₵0.25/kWh, the total cost reduction is improved by 1.88% when the number of EVs increases from 10 to 20, but it only improves by 0.49% when EV quantity increases from 50 to 60.

The battery depreciation cost is another critical factor. As shown in Figure 12, the effectiveness of cost reduction induced by the proposed V2M system improves as the depreciation cost decrease. The red line with ₵0/kWh shows the theoretically largest cost reduction. The current battery depreciation cost is between ₵0.25/kWh and ₵0.5/kWh. However, battery cost has already fallen by 80% from 2013 to 2017, and it is anticipated to be further reduced with battery technology improvement [37]. Therefore, the proposed V2M system could play a greater role in energy demand flexibility improvement for DR in manufacturing facilities in the future.

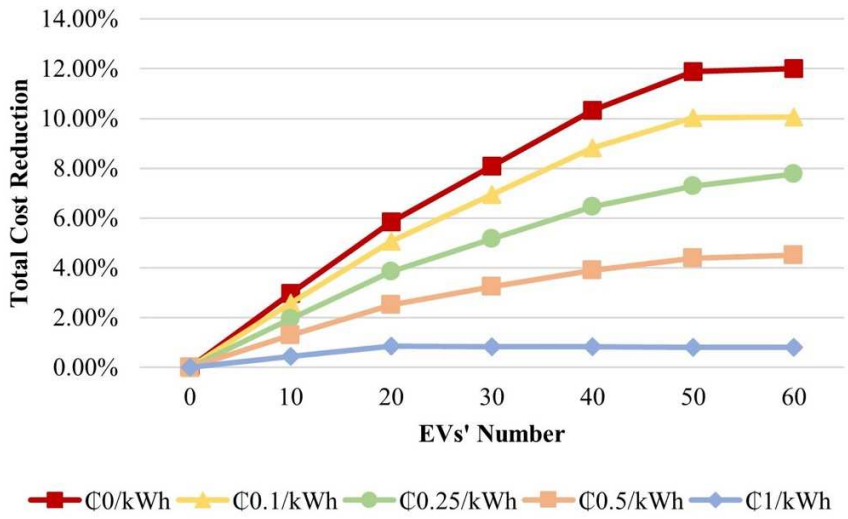

Figure 12. The total cost reduction of the system under different EV quantities and battery depreciation costs.

4 Conclusions and future work

In this paper, the framework of V2M energy sharing system is proposed, which can significantly improve the energy demand flexibility in manufacturing facilities and reduce the energy cost for manufacturers under DR. The interconnection among various manufacturing resources, impacts of production on HVAC load, multi-directional energy flows, and dynamic RTPs are jointly considered in the system model. A MINLP problem is formulated to obtain the optimal V2M-based DR scheme. The case studies results show that, compared to traditional manufacturing DR scheme, the proposed approach can enhance the energy demand flexibility by up to 6.5 times and further reduce the energy cost by 4.7% to 6.9%.

As the first few studies considering the energy demand flexibility in manufacturing facilities for DR, this paper provides a foundation for future research for practical DR schemes towards sustainable manufacturing. For example, the effect of the V2M on the power grid stability and reliability improvement should be further investigated and evaluated. In addition, the impacts of other measures to improve energy demand flexibility, such as renewable energy and building thermal mass, on manufacturing DR effectiveness should be investigated. Furthermore, the most advanced information technologies, such as internet of things and cyber-physical systems, could be integrated into the energy sharing system to support intelligent automatic control.

Acknowledges

The authors sincerely appreciate the funding support from the U.S. Department of Energy under Grant Number DE-EE0009714.

References

[1] K. Wohlfarth, E. Worrell, and W. Eichhammer, "Energy efficiency and demand response – two sides of the same coin?," *Energy Policy*, vol. 137, p. 111070, Feb. 2020, doi: 10.1016/j.enpol.2019.111070.

[2] M. Fleschutz, M. Bohlayer, M. Braun, G. Henze, and M. D. Murphy, "The effect of price-based demand response on carbon emissions in European electricity markets: The importance of adequate carbon prices," *Appl. Energy*, vol. 295, p. 117040, Aug. 2021, doi: 10.1016/j.apenergy.2021.117040.

[3] W. Zhong, S. Xie, K. Xie, Q. Yang, and L. Xie, "Cooperative P2P Energy Trading in Active Distribution Networks: An MILP-Based Nash Bargaining Solution," *IEEE Trans. Smart Grid*, pp. 1–1, 2020, doi: 10.1109/TSG.2020.3031013.

[4] W. Zhong, K. Xie, Y. Liu, S. Xie, and L. Xie, "Nash Mechanisms for Market Design based on Distribution Locational Marginal Prices," *IEEE Trans. Power Syst.*, pp. 1–1, 2022, doi: 10.1109/TPWRS.2022.3152517.

[5] L. P. Qian, Y. J. A. Zhang, J. Huang, and Y. Wu, "Demand Response Management via Real-Time Electricity Price Control in Smart Grids," *IEEE J. Sel. Areas Commun.*, vol. 31, no. 7, pp. 1268–1280, Jul. 2013, doi: 10.1109/JSAC.2013.130710.

[6] U.S. Energy Information Administration, "Annual Energy Outlook 2020," 2020.

[7] F. Dababneh and L. Li, "Integrated Electricity and Natural Gas Demand Response for Manufacturers in the Smart Grid," *IEEE Trans. Smart Grid*, vol. 10, no. 4, pp. 4164–4174, Jul. 2019, doi: 10.1109/TSG.2018.2850841.

[8] S. Ma, Y. Zhang, Y. Liu, H. Yang, J. Lv, and S. Ren, "Data-driven sustainable intelligent manufacturing based on demand response for energy-intensive industries," *J. Clean. Prod.*, vol. 274, p. 123155, Nov. 2020, doi: 10.1016/j.jclepro.2020.123155.

[9] L. Yun, S. Ma, L. Li, and Y. Liu, "CPS-enabled and knowledge-aided demand response strategy for sustainable manufacturing," *Adv. Eng. Informatics*, vol. 52, p. 101534, Apr. 2022, doi: 10.1016/j.aei.2022.101534.

[10] F. Dababneh, L. Li, R. Shah, and C. Haefke, "Demand Response-Driven Production and Maintenance Decision-Making for Cost-Effective Manufacturing," *J. Manuf. Sci. Eng.*, vol. 140, no. 6, Jun. 2018, doi: 10.1115/1.4039197.

[11] R. Lu, R. Bai, Y. Huang, Y. Li, J. Jiang, and Y. Ding, "Data-driven real-time price-based demand response for industrial facilities energy management," *Appl. Energy*, vol. 283, p. 116291, Feb. 2021, doi: 10.1016/j.apenergy.2020.116291.

[12] Z. Sun, L. Li, and F. Dababneh, "Plant-level electricity demand response for combined manufacturing system and heating, venting, and air-conditioning (HVAC) system," *J.*

Clean. Prod., vol. 135, pp. 1650–1657, Nov. 2016, doi: 10.1016/j.jclepro.2015.12.098.
[13] L. Yun, L. Li, and S. Ma, "Demand response for manufacturing systems considering the implications of fast-charging battery powered material handling equipment," *Appl. Energy*, vol. 310, p. 118550, Mar. 2022, doi: 10.1016/j.apenergy.2022.118550.
[14] S. Paul and N. P. Padhy, "Real-Time Bilevel Energy Management of Smart Residential Apartment Building," *IEEE Trans. Ind. Informatics*, vol. 16, no. 6, pp. 3708–3720, Jun. 2020, doi: 10.1109/TII.2019.2941739.
[15] W. Zhong, K. Xie, Y. Liu, C. Yang, and S. Xie, "Multi-Resource Allocation of Shared Energy Storage: A Distributed Combinatorial Auction Approach," *IEEE Trans. Smart Grid*, vol. 11, no. 5, pp. 4105–4115, Sep. 2020, doi: 10.1109/TSG.2020.2986468.
[16] X. Zhang, G. Hug, J. Z. Kolter, and I. Harjunkoski, "Demand Response of Ancillary Service From Industrial Loads Coordinated With Energy Storage," *IEEE Trans. Power Syst.*, vol. 33, no. 1, pp. 951–961, Jan. 2018, doi: 10.1109/TPWRS.2017.2704524.
[17] H. Cui and K. Zhou, "Industrial power load scheduling considering demand response," *J. Clean. Prod.*, vol. 204, pp. 447–460, Dec. 2018, doi: 10.1016/j.jclepro.2018.08.270.
[18] J. Mullan, D. Harries, T. Bräunl, and S. Whitely, "The technical, economic and commercial viability of the vehicle-to-grid concept," *Energy Policy*, vol. 48, pp. 394–406, Sep. 2012, doi: 10.1016/j.enpol.2012.05.042.
[19] Y. Zhou, S. Cao, J. L. M. Hensen, and A. Hasan, "Heuristic battery-protective strategy for energy management of an interactive renewables–buildings–vehicles energy sharing network with high energy flexibility," *Energy Convers. Manag.*, vol. 214, p. 112891, Jun. 2020, doi: 10.1016/j.enconman.2020.112891.
[20] C. Liu, K. T. Chau, D. Wu, and S. Gao, "Opportunities and Challenges of Vehicle-to-Home, Vehicle-to-Vehicle, and Vehicle-to-Grid Technologies," *Proc. IEEE*, vol. 101, no. 11, pp. 2409–2427, Nov. 2013, doi: 10.1109/JPROC.2013.2271951.
[21] D. T. Nguyen and L. B. Le, "Joint Optimization of Electric Vehicle and Home Energy Scheduling Considering User Comfort Preference," *IEEE Trans. Smart Grid*, vol. 5, no. 1, pp. 188–199, Jan. 2014, doi: 10.1109/TSG.2013.2274521.
[22] H. Turker and S. Bacha, "Optimal Minimization of Plug-In Electric Vehicle Charging Cost With Vehicle-to-Home and Vehicle-to-Grid Concepts," *IEEE Trans. Veh. Technol.*, vol. 67, no. 11, pp. 10281–10292, Nov. 2018, doi: 10.1109/TVT.2018.2867428.
[23] C. Pang, P. Dutta, and M. Kezunovic, "BEVs/PHEVs as Dispersed Energy Storage for V2B Uses in the Smart Grid," *IEEE Trans. Smart Grid*, vol. 3, no. 1, pp. 473–482, Mar. 2012, doi: 10.1109/TSG.2011.2172228.
[24] A. Buonomano, "Building to Vehicle to Building concept: A comprehensive parametric and sensitivity analysis for decision making aims," *Appl. Energy*, vol. 261, p. 114077, Mar. 2020, doi: 10.1016/j.apenergy.2019.114077.
[25] J. Li and S. M. Meerkov, *Production systems engineering*. Springer Science & Business Media, 2008.
[26] U.S. Energy Information Administration, "Manufacturing Energy Consumption Survey (MECS)," Washington DC., U.S., 2002. [Online]. Available: https://www.eia.gov/consumption/manufacturing/index.php
[27] Z. Zhang, J. Wang, and X. Wang, "An improved charging/discharging strategy of lithium batteries considering depreciation cost in day-ahead microgrid scheduling," *Energy Convers. Manag.*, vol. 105, pp. 675–684, Nov. 2015, doi: 10.1016/j.enconman.2015.07.079.

[28] I. Asadi, P. Shafigh, Z. F. Bin Abu Hassan, and N. B. Mahyuddin, "Thermal conductivity of concrete – A review," *J. Build. Eng.*, vol. 20, pp. 81–93, Nov. 2018, doi: 10.1016/j.jobe.2018.07.002.
[29] timeanddate, "Past Weather in New York, New York, USA — December 2020."
[30] A. Ouammi, "Peak load reduction with a solar PV-based smart microgrid and vehicle-to-building (V2B) concept," *Sustain. Energy Technol. Assessments*, vol. 44, p. 101027, Apr. 2021, doi: 10.1016/j.seta.2021.101027.
[31] Ford, "Ford intelligent backup power." https://www.ford.com/trucks/f150/f150-lightning/features/intelligent-backup-power/ (accessed Jun. 09, 2022).
[32] A. O. David and I. Al-Anbagi, "EVs for frequency regulation: cost benefit analysis in a smart grid environment," *IET Electr. Syst. Transp.*, vol. 7, no. 4, pp. 310–317, Dec. 2017, doi: 10.1049/iet-est.2017.0007.
[33] "ENERGY MARKET & OPERATIONAL DATA," *NYISO*, 2021.
[34] A. Kathirgamanathan *et al.*, "Towards standardising market-independent indicators for quantifying energy flexibility in buildings," *Energy Build.*, vol. 220, p. 110027, Aug. 2020, doi: 10.1016/j.enbuild.2020.110027.
[35] L. Gan, U. Topcu, and S. H. Low, "Optimal decentralized protocol for electric vehicle charging," *IEEE Trans. Power Syst.*, vol. 28, no. 2, pp. 940–951, 2013, doi: 10.1109/TPWRS.2012.2210288.
[36] E. L. Karfopoulos and N. D. Hatziargyriou, "A multi-agent system for controlled charging of a large population of electric vehicles," *IEEE Trans. Power Syst.*, vol. 28, no. 2, pp. 1196–1204, 2013, doi: 10.1109/TPWRS.2012.2211624.
[37] BloombergNEF, "Electric Vehicle Outlook 2021," 2021.